Effects of an Amphiphilic Graft Copolymer on an Oil–Continuous Microemulsion. Viscosity, Droplet Size, and Phase Behavior

ARTICLE *in* THE JOURNAL OF PHYSICAL CHEMISTRY B · NOVEMBER 1999

Impact Factor: 3.3 · DOI: 10.1021/jp991782p

4 AUTHORS, INCLUDING:

Per Hansson
Uppsala University
66 PUBLICATIONS **2,481** CITATIONS

SEE PROFILE

Effects of an Amphiphilic Graft Copolymer on an Oil−Continuous Microemulsion. Viscosity, Droplet Size, and Phase Behavior

Anna Holmberg, Per Hansson, Lennart Piculell,* and Per Linse

Physical Chemistry 1, Center for Chemistry and Chemical Engineering, University of Lund, P.O. Box 124, S-221 00 Lund, Sweden

Received: June 2, 1999; In Final Form: October 5, 1999

The effects of a graft copolymer on a water/AOT/cyclohexane oil−continuous microemulsion has been studied (AOT = sodium bis(2-ethylhexyl) sulfosuccinate). The polymer consists of a hydrophobic poly(dodecyl methacrylate) backbone with hydrophilic poly(ethylene glycol) monomethyl ether side chains. The polymer stabilizes the microemulsion phase slightly with respect to added water, and destabilizes it with respect to added cyclohexane. The average number of water molecules per droplet was determined by the time-resolved fluorescence quenching technique. The graft copolymer affects the microemulsion by increasing the size of the water droplets. The importance of droplet size and side chain-to-droplet stoichiometry for the viscosity has been examined. A maximum in the viscosity was obtained when the droplet concentration was increased progressively and the polymer concentration was kept constant. The largest viscosity enhancement was obtained for the largest droplet sizes.

Introduction

Mixtures of amphiphilic polymers and surfactants have been extensively studied. Most of the research has concerned water-soluble polymers and their interactions with surfactants in aqueous solution.[1,2] Hydrophobically modified water-soluble polymers (HMWSP) are widely studied because of their practical importance in various industrial applications. An HMWSP consists of a water-soluble backbone modified by hydrophobic units that are attached either as side chains (in graft copolymers) or as end caps (in block copolymers) to the backbone. Added surfactants may have a large influence on the rheology and phase behavior of aqueous solutions of HMWSP.[3−13] HMWSP/surfactant mixtures are therefore of use in applications where it is necessary to control rheology and colloidal stability.

Studies of the inverse type of system, i.e., "hydrophilically modified" oil-soluble polymers in oil−continuous surfactant systems, are much scarcer. It is of fundamental interest to study such mixtures and to explore analogies between oil−continuous and water−continuous surfactant systems mixed with associating polymers. Research in this field will give knowledge on how to modify structure and rheology in oil−continuous surfactant systems.

We have in a previous study synthesized a graft copolymer with hydrophilic poly(ethylene glycol) monomethyl ether (MPEO) side chains grafted onto a hydrophobic poly(dodecyl methacrylate) (PDMA) backbone (see Figure 1).[14] The side chains are water soluble and the nonmodified PDMA was found to be soluble in cyclohexane. We found that the PDMA-*g*-PEO graft copolymer was soluble neither in cyclohexane nor in water, but quite soluble in water/AOT/cyclohexane oil−continuous microemulsions (AOT = sodium bis(2-ethylhexyl) sulfosuccinate). An oil−continuous microemulsion consists of nanometer sized spherical water droplets which are stabilized by surfactants such as the anionic AOT.[15] The size of the droplets is controlled by the molar ratio of water to surfactant, w_0. The number density of the droplets depends on w_0 and on the weight fraction of droplets (water + surfactant), c_d, in the microemulsion.

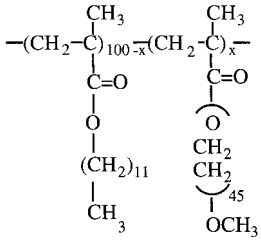

Figure 1. Structure of hydrophilically modified poly(dodecyl methacrylate). x is the number of PEO chains per 100 monomers.

The PDMA backbone of our graft copolymer is soluble in the microemulsion at certain compositions, but it causes phase separation into two clear phases when the concentration of droplets becomes too large. When the graft copolymer is dissolved in a water/AOT/cyclohexane oil−continuous microemulsion, it gives rise to an increase in the viscosity. The relative increase in viscosity depends on the characteristics of the microemulsion and can vary by 1 order of magnitude depending on the volume ratios of AOT, water, and cyclohexane.[14] We attribute the enhanced viscosity to the formation of a network where the backbone of the polymer is dissolved in the oil−continuous phase and the side chains are anchored into the water droplets. We know of no other study of a hydrophilically modified graft copolymer in an oil−continuous system, although there have been reports concerned with amphiphilic triblock copolymers.[16−27]

In the present work we have studied in detail how our graft copolymer affects oil−continuous microemulsions. We have looked at the effects of the polymer on the phase boundary between the oil−continuous microemulsion and the two-phase area in the ternary phase diagram of AOT, water, and cyclohexane. The dependence of the viscosity on the side chain-to-

* Corresponding author.

10.1021/jp991782p CCC: $18.00
Published on Web 11/19/1999

droplet ratio in the microemulsion/copolymer system has been studied in three series of microemulsions with different w_0 values. The polymer concentration was kept constant while the droplet concentration was varied. The water droplet sizes have been estimated by time-resolved fluorescence quenching with and without added polymer.

Experimental Section

Chemicals. Dodecyl methacrylate (DMA) monomers were purified by passing them through a column of basic alumina (BDH, active basic, Brockman Grade 1). 2,2′-Azobis(isobutyronitrile) (AIBN, Merck, 97%), potassium methylate (Merck, 97%), isobutyric acid (BDH, 99%), and toluene (p.a.) were used without further purification. Poly(ethylene glycol) monomethyl ethers (MPEG) with $M_n = 2000$ (Aldrich-Chemie) were used as received. AOT (Sigma, 99%) and cyclohexane (Merck, p.a) were used as delivered. The hydroscopic AOT was stored in a desiccator. Millipore water was used in the microemulsions. Polystyrene standard (Shodex), tetrahydrofuran (HPLC grade, Fisher), and toluene (HPLC grade FSA) were used for MALLS/GPC measurements. 1,3,6,8-Pyrenetetrasulfonic acid tetrasodium salt (PTSA) and potassium iodide (Merck, suprapur) were used as the probe/quencher pair in the fluorescence decay measurements.

Polymer Synthesis. The synthesis of the graft copolymer has been described in detail earlier.[14] Here we give a brief description of the procedure. The backbone polymer was synthesized by radical polymerization of DMA in toluene with AIBN as the initiator. The polymer was purified by repeated precipitation from toluene/methanol and was subsequently dried in a vacuum. Monofunctional PEO was grafted onto PDMA as described by Wesslén et al.[28] Potassium methylate was added to a toluene solution of MPEG. The mixture was refluxed and methanol was distilled off. The MPEO−alkoxide solution was mixed with a toluene solution of the backbone polymer. The solution was refluxed under nitrogen. As the grafting was carried out in dilute homogeneous solution, the grafts can be assumed to be randomly distributed along the backbone.[29] The efficiency of the grafting onto the dodecyl methacrylate backbone was found to be low, presumably due to steric hindrance. The reaction was stopped by neutralizing the reaction mixture with isobutyric acid. The crude polymer was reprecipitated twice from toluene/diethyl ether, dried, redissolved in THF, and precipitated by addition of water. The solution was poured into a dialysis bag and dialyzed against water to remove unreacted MPEO.

Polymer Characterization. The backbone polymer and the graft copolymer were characterized by NMR. The degree of substitution of the graft copolymer was calculated from ^{1}H NMR spectra at ambient temperature in $CDCl_3$ by integrating and comparing resonance signals from the methoxy and oxymethylene groups in the MPEO grafts with characteristic signals from the backbone.

The molecular weight and the mean square radius of gyration were obtained by GPC/light scattering. Light scattering was measured at 632.8 nm on a Dawn F MALLS photometer (Wyatt Technology, Santa Barbara, CA) equipped with a 5 mW He−Ne linearly polarized laser. Pure toluene filtered through a 0.02 μm filter (Whatman) with a known Rayleigh ratio was used to calibrate the photometer. The GPC setup included four Waters Styragel HR columns (500 Å, 103 Å, 104 Å, and mixed bed) coupled in series. A Wyatt/Optilab 903 interferometric refractometer, working at the same wavelength as the light-scattering laser, was used as a mass-sensitive detector. A polystyrene standard with a molecular weight less than 50 000 was used for normalization of the photometer detectors. The measurements were made at 25 °C with tetrahydrofuran as mobile phase, which had been filtered twice through a 0.22 μm Millipore filter. All samples were filtered through a 0.2 μm Millipore filter. The amount of substance injected into the GPC system was 0.78−1.12 mg in 200 μL of solvent. Each reported value is an average of three individual measurements.

Light scattering data were evaluated by using the software Astra supplied by Wyatt Technology. The molecular weight and the radius of gyration were obtained from a Debye plot of $R(\theta)/Kc$ vs $\sin^2(\theta/2)$ through an extrapolation to zero concentration and zero angle. Here $R(\theta)$ is the excess Raleigh ratio, c is the concentration of the macromolecule, and θ is the scattering angle. K is an optical constant equal to $2\pi^2 n_o^2 (dn/dc)^2 2\lambda_0^{-4} N_A^{-1}$, where n_0 is the refractive index of the solvent at the incident wavelength (λ_0), dn/dc is the refractive index increment and N_A is Avogadro's constant. In extrapolating the scattering data to zero angle, a first-order fit was used of data from at least 11 scattering angles. The second virial coefficient was put to zero. (The second term in the virial expansion may generally be neglected at the low concentrations used in chromatographic separations.) The refractive index increment of the backbone polymer was determined using the software DNDC supplied by Wyatt Technology. A series of five different concentrations of the polymer was injected into the RI detector. The change in refractive index dn was measured, and dn/dc was calculated to be 0.070 ± 0.002 mL/g. The same value was used for the graft copolymer, since the limited amount of this polymer precluded a dn/dc determination. This value was found to be consistent with the known injected mass.

Phase Behavior. Microemulsion samples in the one-phase area close to the phase boundary were prepared with and without 10 g/dm^3 polymer. The samples were then diluted by small portions of water until the two-phase area was reached. The phase boundary was detected by visual inspection of the samples in normal light and between crossed polars. Another set of samples with compositions near the oil corner of the one phase area was prepared, and these samples were diluted with oil until two phases appeared.

Viscosity. Measurements for the determination of the intrinsic viscosity of the backbone polymer in cyclohexane were performed on an Ubbelohde Capillary Viscometer (Schott Geräte) with a capillary diameter of 0.46 mm. Samples were prepared in cyclohexane in a concentration range from 0.5 to 16.0 g/dm^3. The capillary was placed in a temperature-controlled water bath. The measurements were made at 20 °C after an equilibration time of 15 min. Each measurement was repeated until three values differing less than 0.1% had been obtained.

The viscosities of microemulsion and microemulsion/copolymer samples were measured on a Carri-Med CSL controlled stress rheometer with a cone and plate geometry. A solvent trap filled with microemulsion was used to avoid solvent evaporation, and the temperature was controlled by a Peltier element. The measurements were done in the shear stress sweep mode. Sixteen different microemulsion compositions were prepared and stirred for 1 day at room temperature. Then, 10 g/dm^3 of copolymer was added to each of the microemulsions, which were stirred for two more days until they became transparent. The viscosities of the microemulsions and of the microemulsion/copolymer samples were measured at 15, 20, and 25 °C.

SAXS. Small-angle X-ray scattering was used to determine the structures of the phase-separated samples. The measurements were performed on a Kratky compact small angle system

equipped with a position sensitive detector (OED 50 M Braun, Graz, Austria) containing 1024 channels. The sample-to-detector distance was 277 nm, and the wavelength was 1.54 Å. The temperature was kept constant at 20 °C with a Peltier element.

Fluorescence Quenching. The fluorescence decay data were collected with the single-photon counting (SPC) technique. A detailed description of the technique and the experimental setup is given elsewhere.[30] All measurements were performed at 20 °C in closed quartz cuvettes. The fluorescence from the probe was selected by using an interference filter (400 ± 5 nm) following excitation at 325 nm. The probe and quencher used in the experiments were PTSA and potassium iodide, respectively.

The fluorescence intensity $I(t)$ after a short pulse at time $t = 0$ can be described by the Infelta−Tachiyia equation[31,32]

$$I(t) = I_0 \exp(-A_1 t + A_2(\exp(-A_3 t) - 1) \qquad (1)$$

where I_0 is the fluorescence intensity at time $t = 0$.

When the probes and quenchers are stationary in the droplets during the lifetime of the probe the total decay is the sum of the emission from excited probes in droplets with 0, 1, 2, 3, ... quenchers. For a Poisson distribution of quenchers among droplets of uniform size, eq 1 can be interpreted as

$$I(t) = I_0 \exp\left(-\frac{1}{\tau_0} + \langle n\rangle(\exp(-k_q t) - 1)\right) \qquad (2)$$

where τ_0 is the lifetime of the probe, k_q is the first-order rate constant for quenching in a droplet and $\langle n\rangle$ is the average number of quenchers per droplet. See the review by Almgren[33] for a detailed description.

In the fitting procedure of the experimental fluorescence decay curves, $I(t)$ in eq 2 was convoluted with the laser pulse response function employing a computer program written for this specific purpose by P.L. Samples without quencher were fitted to a single-exponential function, which gave the fluorescence lifetime τ_0, whereas the full eq 2 was used for samples with quencher. The fitted values of the parameters τ_0, $\langle n\rangle$, and k_q are given in Table 1. In Figure 2 the laser pulse and a typical quenched decay curve are shown together with the fit and the weighted residual (WRES) from the fit. Information about the weighted residual can be found in ref 34.

Results and Discussion

Polymer Characterization. In Figure 3 the reduced viscosity of the backbone polymer in cyclohexane is plotted as a function of the polymer concentration. The intercept obtained from the linear fit corresponds to a limiting viscosity number $[\eta] = 0.048$ dm^3/g. This yields a hydrodynamic radius of 15 nm and an overlap concentration $c^* \approx 21$ g/dm^3 from the relation $c^* \approx 1/[\eta]$. From the GPC/light scattering experiments the weight-average molecular weight of the backbone polymer was found to be 415 000 and the z-average radius of gyration, $R_{g,z}$, was 24 nm.

The GPC chromatogram of the graft copolymer showed a bimodal distribution. However, since a GPC chromatogram obtained just after the synthesis showed only one peak, we believe the bimodal distribution is due to aggregation with time. We have been unable to determine whether this aggregation was of a chemical or a physical nature. The high molecular weight fraction of the polymer distribution contained approximately 12% of the polymer mass. The average molecular weight of the low-molecular fraction alone was 780 000 and $R_{g,z}$ was 33 nm. No effects of the small aggregated fraction of the graft copolymer on the properties relevant to this study were observed. We did not see any change in the viscosity of polymer-containing microemulsions with time, and the diffusion coefficient (measured by NMR) of the polymer in the microemulsion was the same as for a newly synthesized copolymer with the same substitution degree. The degree of grafting calculated from the ^{1}H NMR spectra was 2.7 PEO chains per 100 PDMA monomers.

TABLE 1: Values of τ_0, $\langle n\rangle$, k_q, W_m, Q_m, and N_w^{app} Obtained from the Fits of Eq 2 Convoluted with the Laser Pulse Response Function to the Experimental Fluorescence Decay Data

sample	τ_0 (ns)	$\langle n\rangle$	k_q (1/ns)	Q_m (mM)	W_m (mM)	N_w^{app}
I	9.78	2.29	0.307	2.105	828	900
	9.78	1.93	0.282	1.686	828	947
	9.78	1.40	0.249	1.262	828	918
	9.78	1.23	0.236	0.843	828	1208
	10.18	1.15	0.254	1.060	832	902
	10.18	1.03	0.245	0.795	832	1078
	10.18	0.810	0.233	0.530	832	1272
	10.18	0.420	0.231	0.26	832	1319
I + 0.55% polymer	7.86	2.09	0.143	1.060	832	1640
	7.86	1.94	0.1560	0.795	832	2030
	7.86	1.48	0.0929	0.530	832	2323
	7.86	0.50	0.0898	0.265	832	1570
I + 1.11% polymer	7.61	3.96	0.0820	2.104	828	1558
	7.61	3.36	0.0745	1.686	828	1650
	7.61	2.77	0.0568	1.262	828	1817
	7.61	2.56	0.0535	0.843	828	2514
II	10.30	1.28	0.136	1.059	1686	2038
	10.30	1.02	0.130	0.794	1686	2166
	10.30	0.74	0.127	0.529	1686	2358
	10.30	0.42	0.134	0.265	1686	2672
II + 1.11% polymer	8.48	2.12	0.0481	1.059	1686	3375
	8.48	1.70	0.0450	0.794	1686	3610
	8.48	1.37	0.0393	0.529	1686	4366
	8.48	0.63	0.0452	0.265	1686	4008
II + 2.22% polymer	8.31	2.05	0.0424	1.059	1686	3264
	8.31	1.91	0.0307	0.794	1686	4056
	8.31	1.46	0.0281	0.529	1686	4653
	8.31	0.74	0.0296	0.265	1686	4708

[a] The lifetime, τ_0, of the probe (1,3,6,8-pyrenetetrasulfonic acid tetrasodium salt) was held constant to the value obtained from a single-exponential fit of the corresponding unquenched decay.

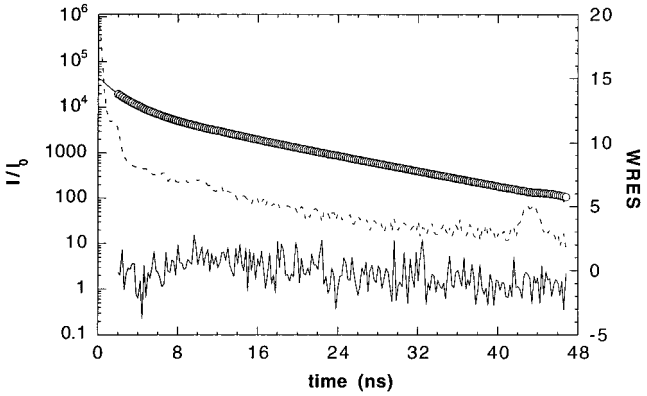

Figure 2. Fluorescence laser pulse curve (broken line) and decay curve (solid line) given together with the fit, ○, and the weighted residual (WRES) from the fit.

Phase Behavior. Results from dilution of microemulsion or microemulsion/copolymer samples with water at 20 °C are shown in Figure 4. The symbols indicate the relative weight proportions of water, oil, and surfactant in the microemulsions at the phase boundary between the oil−continuous microemulsion and the two-phase area. The phase boundaries look almost

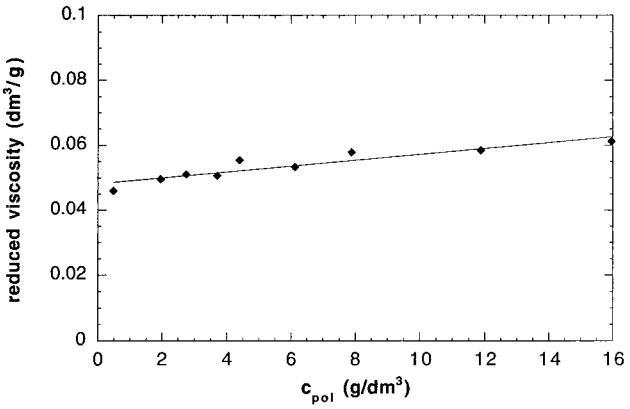

Figure 3. Reduced viscosity of poly(dodecyl methacrylate) in cyclohexane vs polymer concentration at 20 °C.

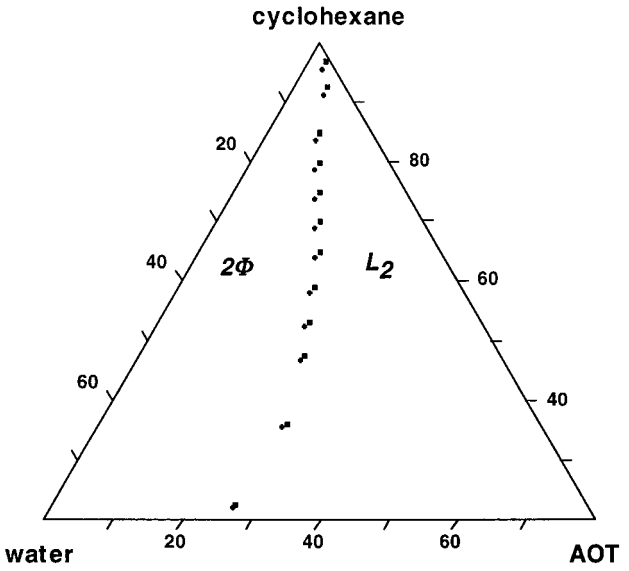

Figure 4. Phase boundaries between the oil−continuous microemulsion phase, L_2, and the two phase area, 2Φ, in the ternary phase diagram AOT/water/cyclohexane in the absence, ■, and in the presence, +, of 1 wt % graft copolymer at 20 °C. The polymer mass is not included in the compositions.

the same at 15 and 25 °C, but an increase in temperature results in a slight expansion of the microemulsion phase.

The main result is that not much happens when the polymer is added to the oil−continuous microemulsion. The microemulsion can take up more water upon polymer addition, i.e., the microemulsion phase becomes slightly, but significantly, larger in the phase diagram. The water uptake with 1% graft copolymer was increased by on average 1.3% at 25 °C, 1.2% at 20 °C, and 1.1% at 15 °C.

When the pure microemulsion was diluted with water, small droplets separated out from the clear phase and fell to the bottom. The phase separation looked different in the microemulsion/copolymer system, which separated into a turbid bottom phase and a clear top phase. The volume of the bottom phase was very small, and it could not be properly separated from the top phase for composition analysis, but it was not birefringent and did not show any structure in a SAXS measurement. NMR of the top phase confirmed that the latter phase still contained polymer.

The nature of the phase separation in AOT water-in-oil microemulsions depends on temperature due to the change in the hydrophilic−lypophilic balance of AOT, which becomes more hydrophilic with increasing temperature.[15] Two types of

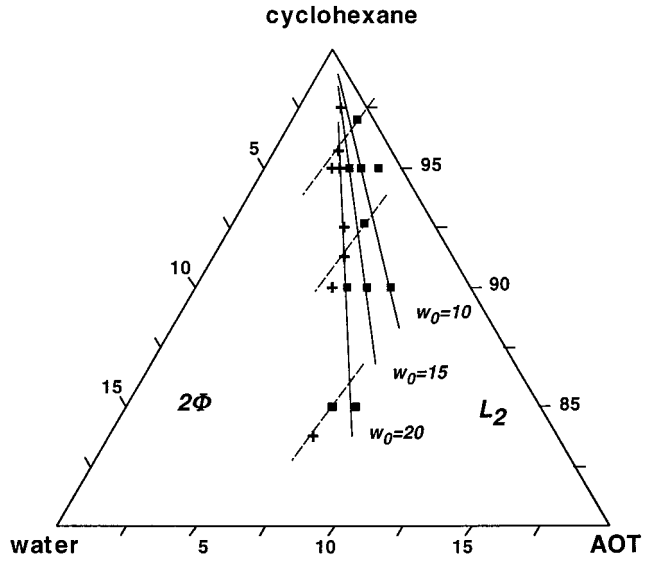

Figure 5. Phase separation of microemulsions containing 1 wt % polymer upon dilution with oil (solid lines) and water (broken lines) at 20 °C and indicated w_0. Key: 2Φ, two phase system; L_2, oil−continuous microemulsion; ■, one-phase samples; +, two-phase samples. The polymer mass is not included in the compositions.

phase separation are observed: (a) At low temperatures water separates out from the L_2 phase, and (b) at high temperature, above the so-called haze point, an opaque AOT- and water-rich phase separates out from oil. Phase boundary a is called the solubilization limit, and the interdroplet attractions are at a minimum, while at phase boundary b there is a strong attractive interaction, leading to droplet clustering.[35]

Samples with pure microemulsion were heated to 50 °C to check the resemblance with the phase separated microemulsion/polymer samples. At this temperature the phase separation looked like the one for the microemulsion/polymer samples. Thus, it is possible that the polymer lowers the haze point in the microemulsion.

When the amount of cyclohexane was less than 40 wt % the microemulsion and the microemulsion/copolymer samples phase separated, upon addition of water, into clear top phases and turbid birefringent bottom phases. SAXS measurements showed that the bottom phases had a lamellar structure in both mixtures. A lamellar phase has been observed before in the ternary phase diagram of AOT, water, and cyclohexane in the presence of small amounts of salt.[36]

To choose samples for the viscosity study we had to examine the dependence of the polymer solubility in the microemulsion on the side chain-to-droplet ratio. While doing this, we found that the polymer/microemulsion system phase separated at a certain point when the oil corner was approached (>97 wt % oil). This type of phase separation did not occur in the ternary mixture without polymer. Samples with 1 wt % polymer were prepared in microemulsions with droplets of different sizes. The size of the droplets is controlled by the molar ratio of water to surfactant, w_0. The polymer/microemulsion samples were diluted with cyclohexane until phase separation occurred; see Figure 5. A clear concentrated isotropic bottom phase separated out (spread out on the walls of the sample container) from a clear solution with low viscosity. The bottom phase thus had a quite low relative volume (ca. 5%) and was much more concentrated than the single-phase solution that existed prior to the addition of cyclohexane. The same type of phase separation was observed also when the oil was changed to isooctane.

Batra et al. also encountered a phase separation upon addition

of oil to an oil−continuous microemulsion containing an amphiphilic copolymer. They studied AOT/water/decane microemulsions containing PEO/PI/PEO triblock copolymers.[19,20] In their case, the lower phase was a high-viscosity fluid, while the upper phase was a clear low-viscosity fluid. This phase separation was explained in terms a finite swelling of the polymer network, and in accordance with this interpretation, the relative volume of the concentrated phase was large close to the phase boundary.[37] This is different from our case, where a small volume of concentrated phase separated out.

Phase separation on dilution has also been seen in water−continuous surfactant systems containing amphiphilic polymers. A mixed solution of HM−EHEC (ethyl (hydroxyethyl) cellulose hydrophobically modified with branched nonylphenol) and sodium dodecyl sulfate (SDS) in water has been reported to phase separate upon dilution with water.[38] Hydrophobically endcapped poly(ethylene oxide) polymer in a nonionic water−continuous system was found to induce an associative phase separation with excess water, both in the lamellar liquid crystalline phase and in the microemulsion phase.[39] In both of these systems, an excess solvent phase separated out from a concentrated polymer phase, and the phase separation was explained by a finite swelling of the polymer matrices, just as in the study of the oil−continuous system by Batra et al.

At present, we have no satisfying mechanism to propose for the phase separation on dilution in our system, which is different from the other cases reported in the literature. Contamination of the oil can surely be ruled out, since we found the effect in two different oils. A similar phase separation may be expected upon adding to a polymer solution a liquid that is miscible with the solvent while being a nonsolvent for the polymer. However, the simple polymer/solvent/nonsolvent mixture is quite different from our system, where the microemulsion is a structured fluid containing two immiscible liquid components in compartments separated by a surfactant layer.

Viscosity. Mixtures of surfactants and hydrophobically modified water-soluble polymers show interesting rheological behavior. When the surfactant concentration is increased gradually at a constant polymer concentration the viscosity increases until it reaches a maximum; on further addition it decreases again.[3,7,8,10,12,40−44] The increase in viscosity is not fully understood, though the formation of mixed micelles between the added surfactant and the hydrophobic groups of the polymer seems to be important. The viscosity decreases when the number of hydrophobes per micelle starts to decrease, i.e., when the concentration of mixed micelles starts to increase, leading to a decreased functionality of the mixed micellar cross-links.[45,46] In the present study, we wished to see if there is a similar effect with hydrophilically modified oil-soluble polymers in oil−continuous systems. We thus mixed the polymer in microemulsions with increasing droplet concentrations for three different droplet sizes, always keeping the polymer concentration constant at 10 g/dm^3. The compositions of the three series of microemulsions investigated by viscometry are shown in Figure 6. It was not possible to extend the measurements to zero droplet concentration since the copolymer is insoluble in pure cyclohexane.

Newtonian viscosities were obtained for all samples measured. The results at 15, 20, and 25 °C are shown in Figure 7a. The viscosity decreases with increasing temperature. Similar temperature dependence was observed in AOT/water/isooctane oil−continuous microemulsions with triblock copolymers.[21] In relation to this, it can be mentioned that the rate of exchange of aqueous solubilizates between AOT stabilized droplets has been found to depend on the temperature. The second-order rate constant for exchange, measured by stopped-flow and continuous- flow techniques, increases with increasing temperature.[47] When the temperature is increased the haze point is approached, the droplet interactions soften and their fusion is facilitated.[15]

To illustrate the effect of the copolymer, we show in Figure 7b the relative viscosity, i.e., the viscosity of the microemulsion/

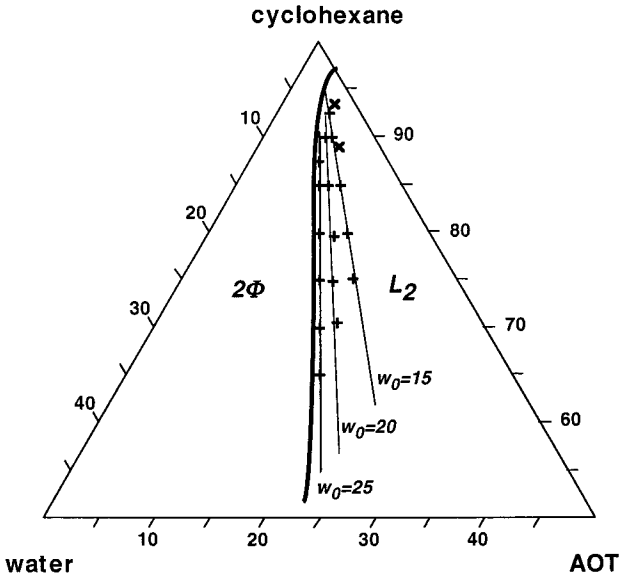

Figure 6. Compositions of microemulsions investigated by viscosity measurements, +, and fluorescence quenching measurements, ×. The fat solid line indicates the phase border.

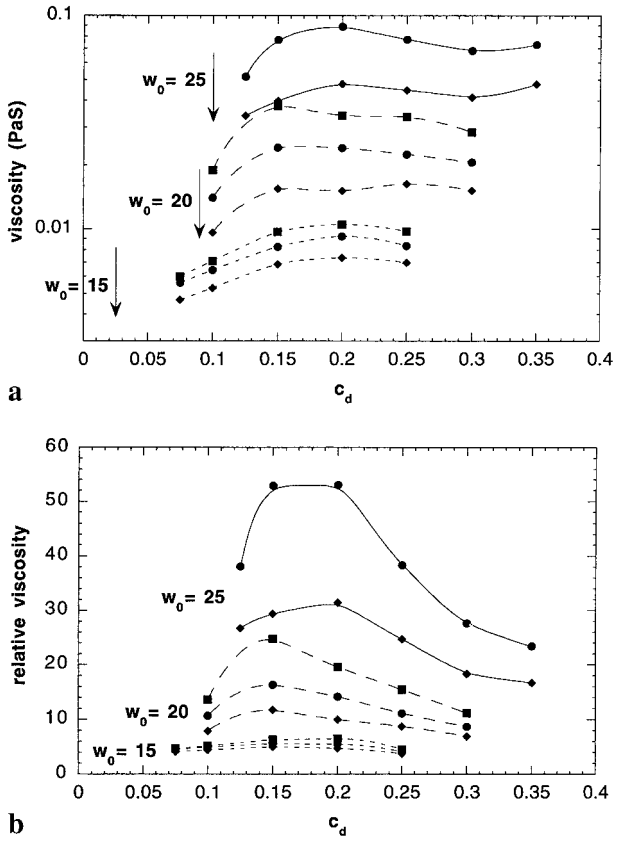

Figure 7. Viscosity (a) and relative viscosity (b) of microemulsions all containing 10 g/dm^3 of copolymer vs the weight fraction of droplets at (◆) 15, (●) 20 and (◆) 25 °C at the indicated w_0. The arrows indicate the limits of the one-phase area at 20 °C. Key: solid lines, $w_0 = 25$; dashed lines, $w_0 = 20$; dotted lines, $w_0 = 15$.

TABLE 2: Composition of Microemulsions Used in the Fluorescence Quenching Measurements

sample	AOT (wt %)	water (wt %)	$C_{12}H_{24}$ (wt %)	w_0	c_d
I	4.65	1.88	93.47	10	0.065
II	7.30	3.73	88.98	12.6	0.11

copolymer samples divided by the viscosity of the polymer-free microemulsion. (The absolute viscosity of the latter obviously increases with an increasing droplet concentration.) As the weight fraction of droplets is increased, the relative viscosity increases and reaches a maximum. When the weight fraction is increased further, the relative viscosity decreases. A maximum was found for all three w_0 values, but the effect was more pronounced with larger droplets (higher w_0 value). We conclude that the copolymer is able to form an interconnecting network in the microemulsion by having the side chains in the water droplets and the backbone in the oil−continuous phase. The bridging points are water droplets that contain side chains from more than one polymer. This network gives rise to an increase in the viscosity. As for the analogous water−continuous systems studied previously, we attribute the viscosity decrease at high droplet concentrations to a decreased functionality of the network. It is interesting that an initial increase appears also in our system, as in the aqueous case. However, the mechanism might be different in the two cases. It must be remembered that in the system studied here, the copolymer is insoluble in the droplet-free oil. Thus, the decrease in viscosity with decreasing droplet concentration may be caused by an increased aggregation preceding the phase separation; in such a process, the branched network structure could be gradually transformed into a structure of more compact disconnected aggregates.

Fluorescence Quenching. Fluorescence quenching was used to obtain microscopic information on the average number of water molecules per droplet in the pure microemulsion and in the microemulsion/copolymer mixtures. Lang et al. have shown, in studies of AOT/water/alkane oil−continuous microemulsions, that this method gives good agreement with measurements made with other techniques such as light scattering and small-angle neutron scattering.[48]

Several combinations of probe and quencher were tested before we finally chose PTSA/I^- as our probe/quencher pair. Verbeeck et al. found that this couple gave an excellent agreement with results from other techniques in the AOT/water/*n*-hexane system.[49] In fact, after testing several different probe/quencher pairs, these authors recommended PTSA/I^- (or PTSA/SCN^-) for the size determination of small w/o microemulsion droplets. It can be mentioned that $Cl_3[Ru(bp)_3]/K_3[Fe(CN)_6]$, used by Howe et al., resulted in a phase separation in our system.[48,50] Furthermore, *N*-cetylpyridinium chloride did not quench effectively either PTSA or 1-pyrenebutyl trimethylammonium ions in the droplets. The latter probe was tested because it has a longer lifetime than the former. As discussed by Almgren et al. the use of a multivalent probe (−4 in the case of PTSA) can lead to errors if the quencher tends to avoid droplets containing the probe.[51] The effect is expected to be important for very small droplets, as indicated also by their measurements. However, for sufficiently large droplets ($w_0 >$ 8) they observed no deviation from the expected behavior.

The compositions of the systems investigated in the present work are indicated in Figure 6. Unfortunately, due to limitations of the method (cf. below), fluorescence measurements could only be performed on samples with relatively small droplet sizes, comparable to the smallest droplet sizes that were investigated by viscometry. Two different microemulsions, **I** and **II** (see Table 2), were prepared with probe concentrations in the range

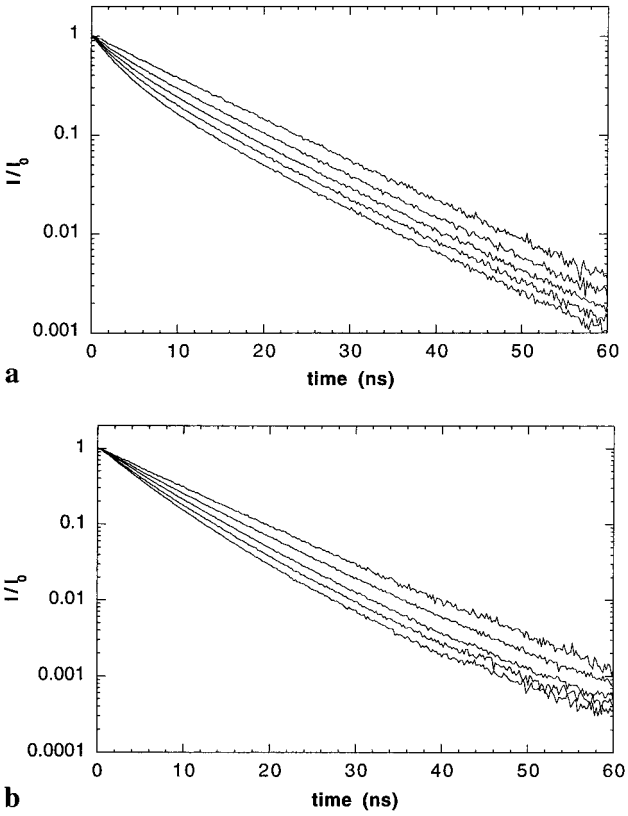

Figure 8. Fluorescence decays for microemulsion **II** (a) and microemulsion **II** with 1.11 wt % polymer (b). The probe concentration was 26.5 μM, and the quencher concentration increased from zero in the top curves to about 1.059 mM in the bottom curves.

0.0265−0.0564 mM. Quencher was added at four different concentrations to each microemulsion. Representative decay curves are shown in Figure 8. Without polymer the concentration of droplets was the same in the two microemulsions and the droplet volume was twice as large in **II** as in **I**. The copolymer was added to each microemulsion at two different concentrations; 0.55 or 1.11 wt % was added to **I**, and 1.11 or 2.22 wt % was added to **II**.

The number concentration of droplets, C_d, and the apparent average number of water molecules per droplet, N_w^{app}, in the microemulsion were calculated for each microemulsion from

$$C_d = \frac{Q_m}{\langle n \rangle} \tag{3}$$

$$N_w^{app} = \frac{W_m}{C_d} \tag{4}$$

where Q_m and W_m are the number concentrations of quencher and water in the microemulsions, respectively. The solubility of water in cyclohexane is 5 mM.[52] Since the total water concentration in the present study was 828 mM or more, the water dissolved in cyclohexane was neglected in the calculations. The calculated values of Q_m,W_m, and N_w^{app} are given in Table 1 together with the values of τ_0, $\langle n \rangle$, and k_q obtained from the fits.

The apparent average number of water molecules per droplet is plotted against the quencher concentration in Figure 9. The results show a decrease in the apparent aggregation number when increasing the quencher concentration. This effect is expected due to the polydispersity of the droplets.[53] Another factor contributing to the observed effect could be a net repulsion

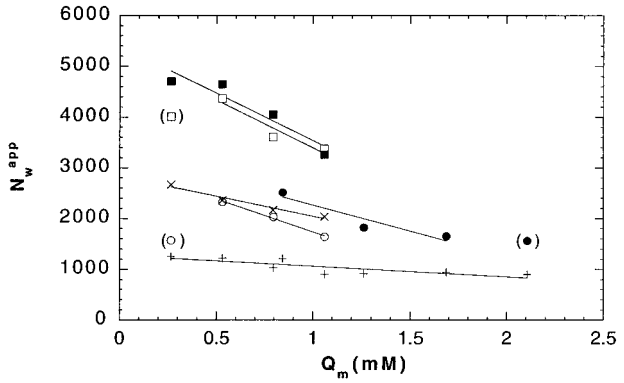

Figure 9. Apparent average number of water molecules, N_w^{app}, per microemulsion droplet vs the quencher concentration, Q_m. Key: +, microemulsion **I**; ○, microemulsion **I** plus 0.55 wt % polymer; ●, microemulsion **I** plus 1.11 wt % polymer; ×, microemulsion **II**; □, microemulsion **II** plus 1.11 wt % polymer; ■, microemulsion **II** plus 2.22 wt % polymer. Solid lines are guides for the eye, and dashed lines show the extrapolation to zero quencher concentration. Points in parentheses were not used in the extrapolation.

between the quenchers (I^-).[54,55] This would lead to a deviation from the Poisson distribution of quenchers among the droplets. However, the effect is probably negligible in the present case due to the high concentration of surfactant ions and counterions in the droplets. The concentration of ions in the droplets is 40 times higher than the iodide concentration in microemulsion **I** and 120 times higher in microemulsion **II**, respectively.

The deviating low aggregation numbers estimated for sample **II** + 1.11% polymer and **I** + 0.55% polymer at the lowest quencher concentration (0.265 mM) are probably an effect of the low degree of quenching in those samples; the quenching is barely observable by simple inspection of the decay curves. The effect is most pronounced for polymer-containing samples due to a slow quenching; cf. Figure 8. The effect is also seen in **II** + 2.22% polymer but not to the same extent. Reduced quenching caused by the polymer has been observed previously in polymer surfactant systems.[45,46,56] In the present system, where the probe and the quencher reside in the water pools, an obstruction from the PEO chains is the most probable explanation.

The size polydispersity of the droplets can be quantified from the dependence of the apparent average aggregation number, N_w^{app}, on the mean number of quenchers per water molecule, η:

$$N_w^{app} = N_w - (\sigma^2/2)\eta + (\kappa_3/5)\eta^2 + ... \quad (5)$$

Here N_w is the weight-average aggregation number (the value of N_w^{app} extrapolated to zero quencher concentration), σ^2 the variance of the weight distribution, and κ_3 the third cumulant.[53,57] Equation 5 was used to analyze the data in Figure 9, neglecting terms of higher order than the linear term. The resulting relative polydispersity in the aggregation number, σ_{N_w}/N_w, is given in Table 3 together with the relative radius polydispersity, σ_r/r. The latter, commonly referred to as the polydispersity index, was calculated from the former using the relations given by Almgren et al.[51] Although the estimates in some cases rely on rather bold extrapolations it is interesting to note that σ_r/r is 0.17−0.18 for microemulsions **I** and **II** both in the presence of and in the absence of the polymer. Thus, the polymer-induced growth does not lead to a change in the relative radius polydispersity within the accuracy of our measurements. We note in this context that there were always, on average, two or more PEO chains per droplet according to our measurements.

TABLE 3: Relative Aggregation Number Polydispersity, σ_{N_w}/N_w, and the Relative Radius Polydispersity, σ_r/r, Calculated Using Eq 5, Neglecting Terms of Higher Order than Linear

sample	σ_{N_w}/N_w	σ_r/r
I	0.49	0.17
I + 0.55% polymer	0.49	0.17
I + 1.11% polymer	0.52	0.18
II	0.53	0.18
II + 1.11% polymer	0.49	0.17
II + 2.22% polymer	0.49	0.17

Even for a random distribution of the chains the fraction of "empty" droplets would then be ≤10%. The values of σ_r/r are similar to those reported by Almgren et al. for AOT/water in octane and dodecane using the same technique, but larger than the value (0.12) from light scattering measured by Ricka et al. in hexane.[51,58] One conclusion from the latter study was that the radius polydispersity was almost independent of w_0 over a wide range.

Average numbers of water molecules per droplet in our samples were obtained by linear extrapolation of the data in Figure 9 to zero quencher concentration, neglecting the deviating points at the lowest quencher concentrations for the polymer-containing samples. For the polymer-free microemulsions, we thus obtained $N_w = 1200$ and 2750 in microemulsions **I** and **II**, respectively. If the droplets are assumed to be monodisperse spheres covered with a monolayer of AOT, the radius of the water pool, r_w, and the AOT surface area, a_{AOT} (i.e., the area occupied by each AOT molecule at the surface of the spherical water domain), can be calculated:

$$r_w = \left(\frac{3N_w V_w}{4\pi}\right)^{1/3} \quad (6)$$

$$a_{AOT} = \frac{w_0 4\pi r_w^2}{N_w} \quad (7)$$

Here V_w represents the molecular volume of water. The obtained values of r_w and a_{AOT} are 20 and 44 Å^2 in microemulsion **I** and 27 and 42 Å^2 in microemulsion **II**, respectively. Note the satisfactory agreement of a_{AOT} for the two droplet sizes. The AOT surface area has previously been found to vary from 40 to 70 Å^2 depending on the type of oil used, the temperature, w_0, and c_d.[48,59−61]

The average number of water molecules per droplet increases with increasing polymer concentration. In Figure 10, N_w is presented both as a function of the polymer concentration (Figure 10a) and as a function of the number of PEO chains per droplet (Figure 10b). In both microemulsions the polymer gives rise to a large increase in N_w already at rather modest PEO contents, and then the effect seems to level off. It might be suspected that the polymer effect would be smaller for larger droplets. Unfortunately, however, we could not investigate this point by our fluorescence method since the quenching rate would be too slow. A trivial increase in droplet size is expected purely from the dissolution of the PEO chains in the water microphase. An increase in the volume of the water microphase at a constant surface area (as implied by the constant surfactant content) must lead to a decrease in the number of droplets and, hence, a decrease in N_w. If it is assumed that the droplets remain spherical, a simple estimate of the volume increase of the water microphase predicts for both microemulsions a nearly linear increase in N_w amounting to ca. 300 at 1% of copolymer—an effect far smaller than that observed in Figure 10. Note that the calculation actually represents an upper limit, since an expected

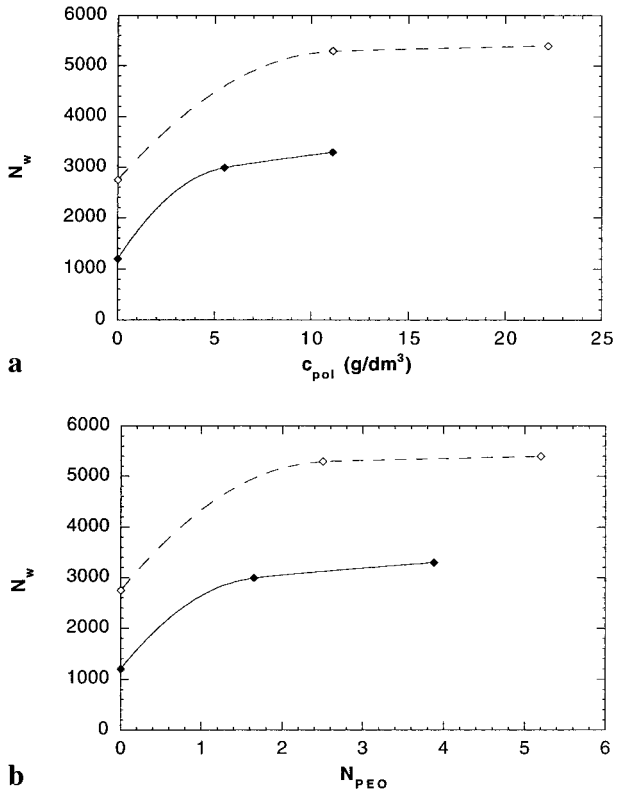

Figure 10. Average number of water molecules per droplet vs the polymer concentration (a) or the average number of PEO chains per droplet (b). Key: ◆, microemulsion **I**; ◇, microemulsion **II**. Lines are guides for the eye.

contribution from the copolymer to the total surface area of the droplets is neglected. It appears then that the larger droplets formed in the presence of the graft copolymer deviate significantly from a spherical shape.

At this point, it is appropriate to consider if the trend in Figure 10 could instead be caused by some possible errors associated with the fluorescence method in the present system. One such effect could be due to a possible clustering of droplets connected by copolymer molecules, which could lead to rapid exchange of quencher and/or probe between the droplets. This effect can be ruled out, however, since the deactivation rate at long times after the excitation event is identical in the absence and in the presence of quencher. This means that there is no migration of the quencher between the droplets during the sampling time (ca. 100 ns). A second type of error may be caused by strong quencher/quencher, quencher/probe, or probe/probe interactions. However, since we have no reason to question the estimates in the pure microemulsion (see above), we need only consider possible effects from the added polymer and the PEO side chains in particular. (Note that interactions of purely electrostatic nature are present also in the absence of polymer.) To test for effects of PEO alone, we made some additional measurements where short PEO chains (PEO600) were added to microemulsion **II**. In contrast with previous results on AOT/decane/water/alcohol pentanol w/o microemulsions but in agreement with results on sodium dodecyl sulfate/water/cyclohexane/pentanol w/o microemulsions, we found an increase of the droplet size on addition of PEO.[62,63] At concentrations up to 10% of the water content, the effect of PEO600 was to increase in the droplet volume by $\leq$30%. However, this effect is considerably smaller than that observed in Figure 10. From the above it seems that the increase in N_w seen in Figure 10 is not an artifact, but a real effect.

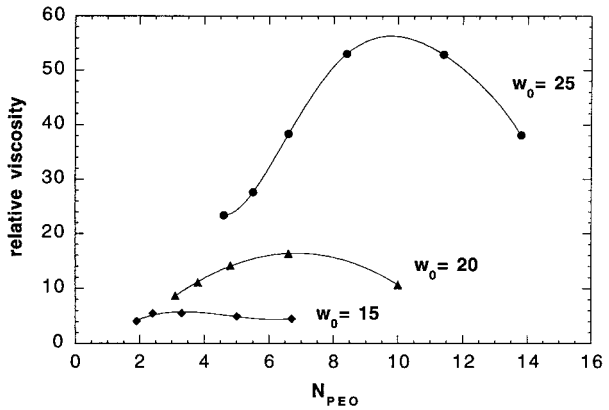

Figure 11. Relative viscosity vs the average number of PEO chains per droplet at 20 °C. Key: ◆, $w_0 = 15$; ▲, $w_0 = 20$; ●, $w_0 = 25$. Lines are guides for the eye.

Moreover, it seems clear that the increase in droplet size is not caused by the PEO side chains alone.

We may use the fluorescence quenching results to obtain microscopic insight into our viscosity results. In Figure 11 the relative viscosity data from Figure 7 are replotted as a function of the number of PEO chains per water droplet. In calculating the latter numbers, we have assumed a value of 42 Å^2 for a_{AOT} and, considering the results in Figure 10b, a doubling of the droplet size (for all w_0 values) in the presence of 10 g/L of copolymer. As pointed out above the effect of the copolymer might be expected to be smaller for larger droplet sizes. However, even if a possible overestimation of the number of PEO chains per water droplet, N_{PEO}, by a factor of $\leq$2 is considered for the largest droplet size, the data in Figure 11 still indicate a significant shift in the maximum in the relative viscosity to larger N_{PEO} values when the size of the droplets is increased, i.e., at higher w_0 values. We have only seen one previous study dealing with the dependence of the viscosity on aggregate size in polymer surfactant systems. In this study the viscosity in aqueous mixtures of surfactant and HM-EHEC was examined. [46] The aggregate size was controlled by mixing SDS with dodecyl trimethylammonium chloride or NaCl. No clear trend in the variation of the viscosity depending on aggregate size could be observed.

Conclusions

In this work we have studied the influence of an amphiphilic graft copolymer on an AOT/water/cyclohexane oil−continuous microemulsion. The graft copolymer is soluble in the microemulsion but is insoluble either in pure water or in pure cyclohexane.

The effect of the polymer on the phase boundary between the L_2-phase and the two-phase area in the ternary phase diagram is small but significant. The nature of the polymer effect is similar to that of raising the temperature above the haze-point: The area of the L_2-phase increases, and on phase separation, a turbid bottom phase separates out from a clear top phase.

Unlike the polymer-free ternary mixture, the polymer/microemulsion system also phase separates upon dilution with oil. The mechanism of this dilution phase separation is not clear, but it appears to be different from the limited swelling previously encountered in other oil−continuous and water−continuous surfactant systems containing amphiphilic polymers.

Added polymer gives rise to a viscosity increase. This effect is ascribed to the formation of an interconnecting network of microemulsion droplets and polymer chains, caused by the

dissolution of PEO side chains in the microemulsion droplets. At this stage, we have no detailed knowledge about the network structure, but it may be assumed that a given polymer chain binds to more than one droplet and vice versa.

A maximum in the relative viscosity appears for all investigated droplet sizes when the weight fraction of droplets is increased at a constant polymer concentration and at a fixed water/surfactant ratio. This observation seems to be new for oil−continuous sytems: we have not seen any similar optimum reported in the literature. Larger droplets lead to a higher relative viscosity and a more pronounced maximum and, also, a larger number of PEO side chains per droplet at the maximum. The viscosity decrease when the droplet concentration is increased above its value at the viscosity maximum suggests that the intermolecular connectivity decreases when the number of PEO side chains per droplet is decreasing. This is similar to the effect of large amounts of surfactant in aqueous solutions of hydrophobically modified polymers. The viscosity decrease on lowering the number of droplets below the value at the maximum is tentatively ascribed to a collapse of the aggregates to denser clusters as the phase boundary is approached. This would result in a less uniform network structure and possibly also in a more rapid exchange of PEO side chains between the droplets.

The fluorescence quenching measurements show that the water droplets in the microemulsion grow considerably upon polymer addition. Simple calculations and direct measurements on short PEO chains show that the effect is too large to be due to the incorporation of the PEO side chains into the droplets. The oil-soluble backbone of the graft copolymer evidently has an important effect on the droplet size, possibly also on its shape. The largest increase in droplet size occurs between zero and approximately two PEO chains per droplet; then the effect levels off. The increase in droplet size does not lead to a change in the relative polydispersity.

Acknowledgment. We are grateful to Ulf Olsson and Bengt Wesslén for discussions and valuable suggestions, and to Mårten Svensson for initial struggles with the fitting programs. This work was supported by grants from The Centre for Amphiphilic Polymers at Lund University (CAP), from the Swedish Research Council for Engineering Sciences (TFR), and from the Schlumberger Stichting Fund. The rheometer was funded by a grant from Nils and Dorthi Troëdsson's Research Foundation.

References and Notes

(1) Piculell, L.; Lindman, B.; Karlström, G. *Phase Behavior of Polymer-Surfactant Systems*; Kwak, J. C. T., Ed.; Marcel Dekker: New York, 1998.
(2) Linse, P.; Piculell, L.; Hansson, P. *Models of Polymer-Surfactant Complexation*; Kwak, J. C. T., Ed.; Marcel Dekker: New York, 1998.
(3) Magny, B.; Iliopoulos, I.; Audebert, R.; Piculell, L.; Lindman, B. *Prog. Colloid Polym. Sci.* **1992**, *89*, 118.
(4) Abrahmsén-Alami, S.; Stilbs, P. *J. Phys. Chem.* **1994**, *98*, 6359.
(5) Annable, T.; Buscall, R.; Ettelaie, R.; Shepherd, P.; Whittlestone, D. *Langmuir* **1994**, *10*, 1060.
(6) Persson, K.; Wang, G.; Olofsson, G. *J. Chem. Soc., Faraday Trans.* **1994**, *90*, 3555.
(7) Kästner, U.; Hoffmann, H.; Dönges, R.; Ehrler, R. *Colloids Surf., A* **1994**, *82*, 279.
(8) Guillemet, F.; Piculell, L. *J. Phys. Chem.* **1995**, *99*, 9201.
(9) Goddard, E. D.; Leung, P. S. *Colloids Surf.* **1992**, *65*, 211.
(10) Gelman, R. A. International Dissolving Pulps Conference. *TAPPI Proc.* **1987**, 159.
(11) Piculell, L.; Thuresson, K.; Ericsson, O. *Faraday Discuss.* **1995**, *101*, 307.
(12) Tanaka, R.; Meadows, J.; Williams, P. A.; Phillips, G. O. *Macromolecules* **1992**, *25*, 1304.
(13) Abdulkadir, J. D.; Steinar, A. C. *Macromolecules* **1990**, *23*, 251.
(14) Holmberg, A.; Piculell, L.; Wesslén, B. *J. Phys. Chem.* **1996**, *100*, 462.
(15) Eastoe, J.; Robinson, B. H.; Steytler, D. C.; Thorn-Leeson, D. *Adv. Colloid Interface Sci.* **1991**, *36*, 1.
(16) Quellet, C.; Eicke, H.-F.; Xu, G.; Hauger, Y. *Macromolecules* **1990**, *23*, 3347.
(17) Eicke, H.-F.; Hofmeier, U.; Quellet, C.; Zölzer, U. *Prog. Colloid Polym. Sci.* **1992**, *90*, 165.
(18) Vollmer, D.; Hofmeier, U.; Eicke, H.-F. *J. Phys. II Fr.* **1992**, *2*, 1677.
(19) Batra, U. Structure and Rheology of AOT Microemulsions: Viscosity Anomalies, Fluctuations and Associating Polymers. Ph.D. Dissertation, Princeton University, 1996.
(20) Batra, U.; Russel, W. B.; Pitsikalis, M.; Sioula, S.; Mays, J. W.; Huang, J. S. *Macromolecules* **1997**, *30*, 6120.
(21) Odenwald, M.; Eicke, H.-F.; Meier, W. *Macromolecules* **1995**, *28*, 5069.
(22) Odenwald, M.; Eicke, H.-F.; Friedrich, C. *Colloid Polym. Sci.* **1996**, *274*, 568.
(23) Zhou, Z.; Hilfiker, U.; Hofmeier, U.; Eicke, H.-F. *Progr. Colloid Polym. Sci.* **1992**, *89*, 66.
(24) Eicke, H.-F.; Gauthier, M.; Hammerich, H. *J. Phys. II Fr.* **1993**, *3*, 255.
(25) Zölzer, U.; Eicke, H.-F. *J. Phys. II Fr.* **1992**, *2*, 2207.
(26) Eicke, H.-F.; Hilfiker, R.; Xu, G. *Helv. Chim. Acta* **1990**, *73*, 213.
(27) Hilfiker, R.; Eicke, H.-F.; Steeb, C.; Hofmeier, U. *J. Phys. Chem.* **1991**, *95*, 1478.
(28) Wesslén, B.; Wesslén, K. B. *J. Polym. Sci., Part A: Polym. Chem.* **1989**, *27*, 3915.
(29) Rempp, P.; Franta, E.; Herz, J.-E. *Adv. Polym. Sci.* **1988**, *86*, 168.
(30) Almgren, M.; Hansson, P.; Mukhtar, E.; van Stam, J. *Langmuir* **1992**, *8*, 2405.
(31) Tachiya, M. *Chem. Phys. Lett.* **1975**, *33*, 289.
(32) Infelta, P. P.; Grätzel, M.; Thomas, J. K. *J. Phys. Chem.* **1974**, *70*, 190.
(33) Almgen, M. *Kinetics of Excited-State Processes in Micellar Media*; Marcel Dekker: New York, 1991.
(34) Almgren, M.; Löfroth, J.-E.; Rydholm, R. *Chem. Phys. Lett.* **1979**, *63*, 265.
(35) Eastoe, J.; Robinson, B. H.; Heenan, R. K. *Langmuir* **1993**, *9*, 2820.
(36) Kunieda, H.; Shinoda, K. *J. Colloid Interface Sci.* **1979**, *70*, 577.
(37) Russel, W. B. Private communication.
(38) Thuresson, K.; Joabsson, F. *Colloids Surf.* **1999**, *151*, 513.
(39) Bagger-Jörgensen, H.; Coppola, L.; Thuresson, K.; Olsson, U.; Mortensen, K. *Langmuir* **1997**, *13*, 4204.
(40) Nyström, B.; Thuresson, K.; Lindman, B. *Langmuir* **1995**, *11*, 1994.
(41) Magny, B.; Iliopoulos, I.; Zana, R.; Audebert, R. *Langmuir* **1994**, *10*, 3180.
(42) Iliopoulos, I.; Wang, T. K.; Audebert, R. *Langmuir* **1991**, *7*, 617.
(43) Iliopoulos, I.; Olsson, U. *J. Phys. Chem.* **1994**, *98*, 1500.
(44) Sarrazin-Cartalas, A.; Iliopoulos, I.; Audebert, R.; Olsson, U. *Langmuir* **1994**, *10*, 1421.
(45) Thuresson, K.; Söderman, O.; Hansson, P.; Wang, G. *J. Phys. Chem.* **1996**, *100*, 4909.
(46) Nilsson, S.; Thuresson, K.; Hansson, P.; Lindman, B. *J. Phys. Chem. B.* **1998**, *102*, 7099.
(47) Fletcher, P. D. I.; Howe, A. M.; Robinson, B. H. *J. Chem. Soc., Faraday Trans*, **1987**, *1*, 985.
(48) Lang, J.; Jada, A.; Malliaris, A. *J. Phys. Chem.* **1988**, *92*, 1946.
(49) Verbeeck, A.; De Schryver, F. C. *Langmuir* **1987**, *3*, 494.
(50) Howe, A. M.; McDonald, J. A.; Robinson, B. H. *J. Chem. Soc., Faraday Trans. 1* **1987**, *83*, 1007.
(51) Almgren, M.; Jóhannsson, R.; Ericsson, J. C. *J. Phys. Chem.* **1993**, *97*, 8590.
(52) Heatley, F. *J. Chem. Soc., Faraday Trans. 1* **1988**, *84*, 343.
(53) Almgren, M.; Löfroth, J.-E. *J. Chem. Phys.* **1982**, *76*, 2734.
(54) Bales, B. L.; Stenland, C. *J. Phys. Chem.* **1993**, *97*, 3418.
(55) Almgren, A.; Hansson, P.; Wang, K. *Langmuir* **1996**, *12*, 3855.
(56) Zana, R.; Binana-Limbelé, W.; Kamenka, N.; Lindman, B. *J. Phys. Chem.* **1992**, *96*, 5461.
(57) Warr, G. G.; Grieser, F. *J. Chem. Soc., Faraday Trans. 1* **1986**, *82*, 1813.
(58) Ricka, J.; Borkovec, M.; Hormeier, U. *J. Chem. Phys.* **1991**, *12*, 8503.
(59) Koltlarchyk, M.; Chen, S.-H.; Huang, J. S. *J. Phys. Chem.* **1982**, *86*, 3273.
(60) Kotlarchyck, M.; Haung, J. S.; Chen, S.-H. *J. Phys. Chem.* **1985**, *89*, 4382.
(61) Eicke, H.-F.; Rehak, J. *Helv. Chim. Acta* **1976**, *59*, 2883.
(62) Suarez, M.-J.; Lévy, H.; Lang, J. *J. Phys. Chem.* **1993**, *97*, 9808.
(63) Lianos, P.; Modes, S.; Staikos, G.; Brown, W. *Langmuir* **1992**, *8*, 1054.